

## Nuclear structure studies in $A \sim 100$ and $A \sim 130$ mass regions

S. Sihotra\*

*Department of Physics, Panjab University, Chandigarh-160014, India*

This paper reports the nuclear structure studies in the mass  $A \sim 100$  and  $A \sim 130$  regions. The investigations were performed in  $^{98,99}\text{Rh}$ ,  $^{99}\text{Pd}$ ,  $^{96}\text{Tc}$ ,  $^{106,107}\text{In}$ , and  $^{129,131}\text{Cs}$  nuclei near the proton ( $Z = 50$ ) and neutron ( $N = 50, 64$ ) shell closures with a view to understand the structural features that result from interplay between single particle and collective degrees of freedom. The nuclei in these regions are characterized by a small quadrupole deformation and soft to gamma deformation at low spins. In order to compare experimental results directly with the theoretical calculations, the experimental spins and level energies have been transformed into the rotating (intrinsic) frame of nucleus. The level schemes have been interpreted in the framework of theoretical model calculations. Configurations assigned to various bands are discussed in the framework of Principal/Tilted Axis Cranking (PAC/TAC) model and the deformed Hartree-Fock and angular momentum projection (PHF) calculations. Level energies and  $B(M1)/B(E2)$  ratios have, on the whole, been reproduced for the assigned configurations. Triaxial deformation in these mass regions has been inferred from the observed rotational-alignment frequencies, staggering behavior, M1 reduced transition probabilities and chiral-twin bands. Another important feature observed in these isotopes is the magnetic dipole bands generated through the shears mechanism. Observation of new E1 transitions linking the opposite-parity bands based on the proton/neutron  $h_{11/2}$  and  $d_{5/2}$  orbitals ( $\Delta l = 3$ ,  $\Delta j = 1$ ,  $\Delta \pi = -1$ ) in  $^{131}\text{Cs}$  and  $^{99}\text{Pd}$  provide fingerprints of possible octupole correlations in these mass-regions.

### 1. Introduction

Nuclei with  $A \sim 100$  in the vicinity of the  $Z = 50$  shell closure have been an interesting subject of study due to existence of both the spherical and deformed shapes. Investigations have revealed diversity in level structures resulting from coupling of  $g_{9/2}$ ,  $d_{5/2}$ ,  $g_{7/2}$ , and  $h_{11/2}$  valence nucleons and the core-excited configurations [1–9]. The proton particle-hole excitations across the major shell gap are energetically possible due to strong proton pair correlations and proton neutron interaction between the spin-orbit partner orbitals. For the nuclei approaching  $Z=50$  from below, the proton Fermi surface lies near the oblate-driving high- $\Omega$  orbitals of the intruder  $\pi g_{9/2}$  subshell. Strongly prolate-driving low- $\Omega$   $\nu h_{11/2}$  subshell orbitals are accessible at low excitation energies for the nuclei receding the

$N=50$  shell closure. The delicate interplay of strongly shape-driving  $\pi g_{9/2}$  and  $\nu h_{11/2}$  orbitals can influence the overall shape of the nucleus and result in  $\gamma$ -soft (triaxial) shapes with the modest deformation. Similarly, in the  $A \sim 130$  mass region [10–13], the active positive parity proton orbitals are  $g_{7/2}$ ,  $d_{5/2}$ , and the  $g_{9/2}$  extruder, and neutron orbitals are  $g_{7/2}$ ,  $d_{5/2}$ ,  $d_{3/2}$ ,  $S_{1/2}$ . In addition, there is the unique parity high- $j$   $h_{11/2}$  intruder orbital in both the proton and neutron valence space, which induce a quadruple nuclear deformation and exert strong and specific shape-driving forces on the core.

Indeed,  $\gamma$ -ray spectroscopic investigations in the odd- $Z$  nuclei in both these regions have revealed collective and non-collective structures representing diverse nuclear shapes. Triaxial deformation in both the  $A \sim 130$  and  $A \sim 100$  mass regions have been inferred from the observed rotational-alignment frequencies, staggering behaviour, and M1 reduced transition probabilities. The relevant intriguing tri-

---

\*Electronic address: [ssihotra@pu.ac.in](mailto:ssihotra@pu.ac.in)

axiality based phenomena such as magnetic rotation and degenerate chiral twin bands have also been reported in these mass regions. Chiral bands have been observed in various odd-A and odd-odd nuclei with multiquasiparticle configurations that have substantial angular momentum components along the three principal axes. Recently the chiral bands in doubly-odd nuclei in  $A \sim 130$  mass region have also been interpreted alternatively in proposed pair truncated shell model (PTSM) [14]. According to PTSM, the level scheme of the  $\Delta I = 1$  doublet bands does not arise from the chiral structure, but from different angular momentum configurations of the unpaired neutron and the unpaired proton, weakly coupled with the quadrupole collective excitations of the even-even core. If we follow the  $\Delta I = 1$  sequence from the ground state, the angular momenta of neutron and proton open and close like scissors and is called chopstick motion. For nuclei in these regions with few nucleons outside closed shell configurations, the terminating states had been observed. Specific noncollective aligned states with the nuclear spin made up completely from angular momentum contribution of the particles and holes in open shells, are able to compete energetically with weakly deformed collective structures in the vicinity of the  $Z=50$  shell closure. As the pair of orbitals with  $\Delta l = 3$  ( $\nu h_{11/2}$  and  $\nu d_{5/2}$ ) and ( $\pi h_{11/2}$  and  $\pi d_{5/2}$ ) lie near the Fermi surface in the  $A = 100$  and  $A = 130$  regions, respectively, signatures of octupole collectivity have also been observed [12, 15].

## 2. Experimental Techniques

Excited states in the nuclei were investigated through in-beam  $\gamma$ -ray spectroscopic techniques following population in the heavy-ion fusion-evaporation reactions. The experiments were performed using heavy ion beams provided by 14 UD Pelletron accelerator at Tata Institute of Fundamental Research (TIFR), Mumbai, and 15 UD Pelletron accelerator at Inter-University Accelerator Centre, New Delhi. The emitted  $\gamma$ -rays were detected with the help of pow-

erful multi-detector arrays (the Indian National Gamma Array (INGA)) consisting of Compton-suppressed clover detectors. The clover detector array due to its higher efficiency at gamma ray energies above 1 MeV is optimum for studies involving excitation of nucleons across the shell gaps, that are likely to result in the occurrence of high energy gamma rays. Further, the use of an array comprising of clover detectors facilitates coincidence polarization measurements, which are crucial to uniquely determine the parity of the state de-exciting via the observed gamma-transition. The analysis of the data collected in the experiments yielded information regarding  $\gamma$ -ray energies, intensities, coincidence relationships, angular correlations, which were necessary to generate the level scheme. The recorded coincidence events from in-beam  $\gamma$ -ray spectroscopic measurements were sorted into two-dimensional  $E_\gamma$ - $E_\gamma$  matrices and  $E_\gamma$ - $E_\gamma$ - $E_\gamma$  cubes using INGASORT [16]. Background-subtracted coincidence spectra were generated and intensity analysis was performed using the computer codes RADWARE [17]. The placement of gamma transitions in the level scheme is based upon their coincidence relationships, energy sums and intensities.

In order to determine the dipole/quadrupole nature of the gamma transitions, directional correlation (DCO) ratios were extracted using an asymmetric matrix made by sorting data with detectors at two different angles. Two dimensional angular correlation matrices between the detectors at  $90^\circ$  and those at  $32^\circ$  and  $148^\circ$  were constructed. For the INGA geometry, the expected values of DCO ratio are typically  $\geq 1.0$  for the quadrupole transitions and  $\leq 0.6$  for the dipole transitions. The clover detector at  $90^\circ$  was used as a Compton polarimeter to determine the electric or magnetic nature of the  $\gamma$ -rays [18]. The integrated polarization directional correlation from oriented nuclei (IPDCO) analysis was done using two asymmetric polarization matrices corresponding to the parallel and perpendicular segments of the clover detector chosen as a Compton

polarimeter (with respect to the emission plane) along one axis and the coincident  $\gamma$ -rays in all the detectors along the other axis.

### 3. Results and Discussion

#### A. The $^{131}\text{Cs}$ nucleus

Excited states in  $^{131}\text{Cs}$  were investigated through in-beam  $\gamma$ -ray spectroscopic techniques following its population in the  $^{124}\text{Sn}(^{11}\text{B}, 4n)$  fusion-evaporation reaction at a beam energy of 46 MeV [12]. The previously known level scheme has been substantially extended up to  $\sim 9$  MeV excitation energy and  $49/2\hbar$  spin with the addition of seven new band structures. The present level scheme, consisting of fifteen bands, exhibits a variety of collective features in this nucleus at intermediate spin. The excitation energies of the observed levels in different bands and the corresponding ratios of transition strengths, *i.e.*,  $B(\text{M1})/B(\text{E2})$ , have been compared with the results of projected deformed Hartree-Fock calculations [19–23] based on various quasiparticle configurations. A strongly coupled band has been reassigned a high-K three quasiparticle  $\pi h_{11/2} \otimes \nu(h_{11/2}d_{3/2})$  configuration based on the properties of this band and that of its new coupled side band. The configurations of these bands are also discussed in the framework of Tilted Axis Cranking model calculations [24] and the systematics of the odd-A Cs isotopes. Additional three energetically closely placed coupled bands have been assigned different unpaired three-quasiparticle configurations. Gamma vibrational bands coupled to the  $\pi h_{11/2}$  and  $\pi g_{7/2}$  single particle configurations have been reported in this nucleus. Observation of new E1 transitions linking the opposite-parity  $\pi h_{11/2}$  and  $\pi d_{5/2}$  bands provides fingerprints of possible octupole correlations. Level energies and  $B(\text{M1})/B(\text{E2})$  ratios have, on the whole, been reproduced for the assigned configurations based on low-lying intrinsic states of one and three unpaired nucleons.

#### B. The $^{129}\text{Cs}$ nucleus

The  $^{122}\text{Sn}(^{11}\text{B}, 4n)$  fusion-evaporation reaction at  $E_{lab} = 60$  MeV was used to populate excited states in  $^{129}\text{Cs}$  and the de-excitations were investigated using in-beam  $\gamma$ -ray spectroscopic techniques [25]. The level scheme of  $^{129}\text{Cs}$  is established up to  $\sim 8$  MeV excitation energy and  $47/2\hbar$  spin. The observed band structures are interpreted for their configurations in the framework of Cranking model calculations and systematic of the neighboring  $^{55}\text{Cs}$  isotopes. A negative-parity  $\Delta I = 1$  coupled band has been assigned the  $\pi h_{11/2} \otimes \nu(h_{11/2})^2$  configuration as solution of the tilted-axis cranking, which coexists with the  $\pi h_{11/2}$  yrast band resulting from the principal-axis cranking. A new band has been identified as  $\gamma$ -vibrational band built on the  $\pi h_{11/2}$  orbital. A pair of strongly coupled positive-parity bands exhibiting similar features have been assigned different unpaired three-quasiparticle configurations involving the  $\pi h_{11/2} \otimes \nu h_{11/2}$  component. The previously identified unfavored signature partners of the  $\pi d_{5/2}$  and  $\pi g_{7/2}$  bands are reassigned as  $\gamma$ -vibrations of the core coupled to the  $\pi g_{7/2}$  single-particle configuration, and the favored signature of the  $\pi d_{5/2}$  band, respectively.

#### C. The $^{106}\text{In}$ nucleus

Excited states in neutron-deficient doubly-odd  $^{106}\text{In}$  were investigated using  $^{78}\text{Se}(^{32}\text{S}, p3n)$  reaction at 125 MeV, with an array of seven Compton suppressed clover detectors [26]. The level scheme has been extended up to 7 MeV of excitation energy for the negative parity states constituting four dipole bands. On the other hand, the positive parity states which mainly exhibit single particle excitations were extended up to 5 MeV. Projected deformed Hartree-Fock calculations were carried out in order to understand the configurations of different bands in this nucleus. A pair of closely spaced dipole bands has been assigned two quasiparticle configurations with  $K^\pi = 4^-$  and  $5^-$  based on  $\pi g_{9/2}$  and  $\nu h_{11/2}$  orbitals, originating from slight rearrangement of the last proton in  $g_{9/2}$  orbital.

#### D. The $^{107}\text{In}$ nucleus

Excited states of the  $^{107}_{49}\text{In}$  nucleus were populated through the  $^{78}\text{Se} (^{32}\text{S}, \text{p}2\text{n})$  fusion-evaporation reaction at beam energy,  $E_{lab} = 125$  MeV [27]. The deexcitations were studied using in-beam  $\gamma$ -ray spectroscopic techniques involving Compton-suppressed clover detector array. The level scheme of  $^{107}\text{In}$  consisting of about seven bands is established up to spin  $\sim 45/2\hbar$  with the addition of 25 new transitions. Spins and parities of various levels have been assigned through the DCO and polarisation measurements. The level structures observed in  $^{107}\text{In}$  have been interpreted in the framework of a microscopic theory based on the deformed Hartree-Fock (HF) and angular momentum projection techniques. Various bands are reproduced in band mixing calculations with the configurations involving high- $\Omega$   $\pi g_{9/2}$  and  $\nu d_{5/2}$  orbits, and low- $\Omega$   $\pi g_{7/2}$ ,  $\nu g_{7/2}$  and  $\nu h_{11/2}$  orbits.

#### E. The $^{99}\text{Pd}$ nucleus

In-beam gamma spectroscopic measurements were carried out to study level structures in  $^{99}\text{Pd}$  nucleus populated through the  $^{75}\text{As} (^{28}\text{Si}, \text{p}3\text{n})$  fusion-evaporation reaction at  $E_{lab} = 120$  MeV [15]. The level structures observed in  $^{99}\text{Pd}$  (Figure 1) have been interpreted in the framework of a microscopic theory based on the deformed Hartree-Fock (HF) and angular momentum projection techniques. Band structures based on the low- $\Omega$   $\nu g_{7/2}$ ,  $\nu d_{5/2}$ , and  $\nu h_{11/2}$  orbitals have been observed. Band structures at higher spins are reproduced with the configurations  $\nu(g_{7/2})^2 \otimes \nu(g_{9/2})^{-1} \otimes \nu(h_{11/2})^2 \otimes \pi(g_{9/2})^6$  with  $K = 5/2^+$ . Various positive and negative parity states, which are energetically more favored with respect to the neighboring ones, are likely to be the maximally aligned states obtained by angular momentum coupling of the  $\pi(g_{9/2})^{-1}$  with  $\nu(g_{7/2})^2, \nu(d_{5/2})^2, \nu(h_{11/2})^2$ . Observation of new E1 transitions linking the opposite-parity  $\nu h_{11/2}$  and  $\nu d_{5/2}$  bands provide fingerprints of possible octupole correlations. The extracted values of the B(E1)/B(E2) ratios for the lower levels in the  $\nu(h_{11/2})$  band are  $\sim$

$10^{-7}$  [ $\text{fm}^{-2}$ ].

#### F. The $^{98,99}\text{Rh}$ , and $^{96}\text{Tc}$ nuclei

The level structures in  $^{98,99}\text{Rh}$ , and  $^{96}\text{Tc}$  nuclei have been investigated through in beam gamma ray spectroscopic techniques following the  $^{75}\text{As} (^{28}\text{Si}, \text{x}p\text{yn})$  fusion-evaporation reaction at  $E_{lab} = 120$  MeV. These investigations were carried out using Indian-National-Gamma-Array (INGA) consisting of Compton-suppressed clover detectors at the Inter-University Accelerator Centre, New Delhi. In case of  $^{98,99}\text{Rh}$ , and  $^{96}\text{Tc}$  the previously reported level schemes have been considerably modified and extended. In the doubly-odd  $^{98}\text{Rh}$  nucleus, new band structures based on isomers have been identified at lower spins and new states below the previously identified  $2^+$  ground state ( $T_{1/2} = 8.5$  m) are identified [29]. Various positive and negative parity states in these nuclei are observed to be energetically more favored with respect to the neighboring ones, and are likely to be the maximally aligned states obtained by angular momentum coupling of the valence particles (holes). Further experiments to identify the isomers in the doubly-odd  $^{98}\text{Rh}$  nucleus are warranted. The spin-parity assignments for most part of the level scheme of  $^{98}\text{Rh}$  is tentative and is based on the assumption of usual multipolarity for the decay transitions, DCO ratios and limited polarization measurements.

The present level scheme of  $^{99}\text{Rh}$  as shown in Figure 2 is built on the  $I^\pi = 1/2^-$  ground state. Five bands labeled B1-B5 could be identified in the present level scheme, which is established up to  $\sim 15$  MeV excitation energy and  $63/2 \hbar$  spin. The low lying band structures are based on the  $\pi(p_{1/2})$  and  $\pi(g_{9/2})$  orbitals which further evolve into high spin structures following  $\nu(h_{11/2})^2$  alignment. In the same region the calculations have been performed by Timar *et. al.* for  $^{101}\text{Rh}$  using cranking Nilsson-Strutinsky formalism [28]. The experimental energies of the observed high-spin bands are compared with the corresponding theoretical values, subtracting the same rigid rotor reference from all of them. The yrast positive parity band at high spin is calculated to have configura-



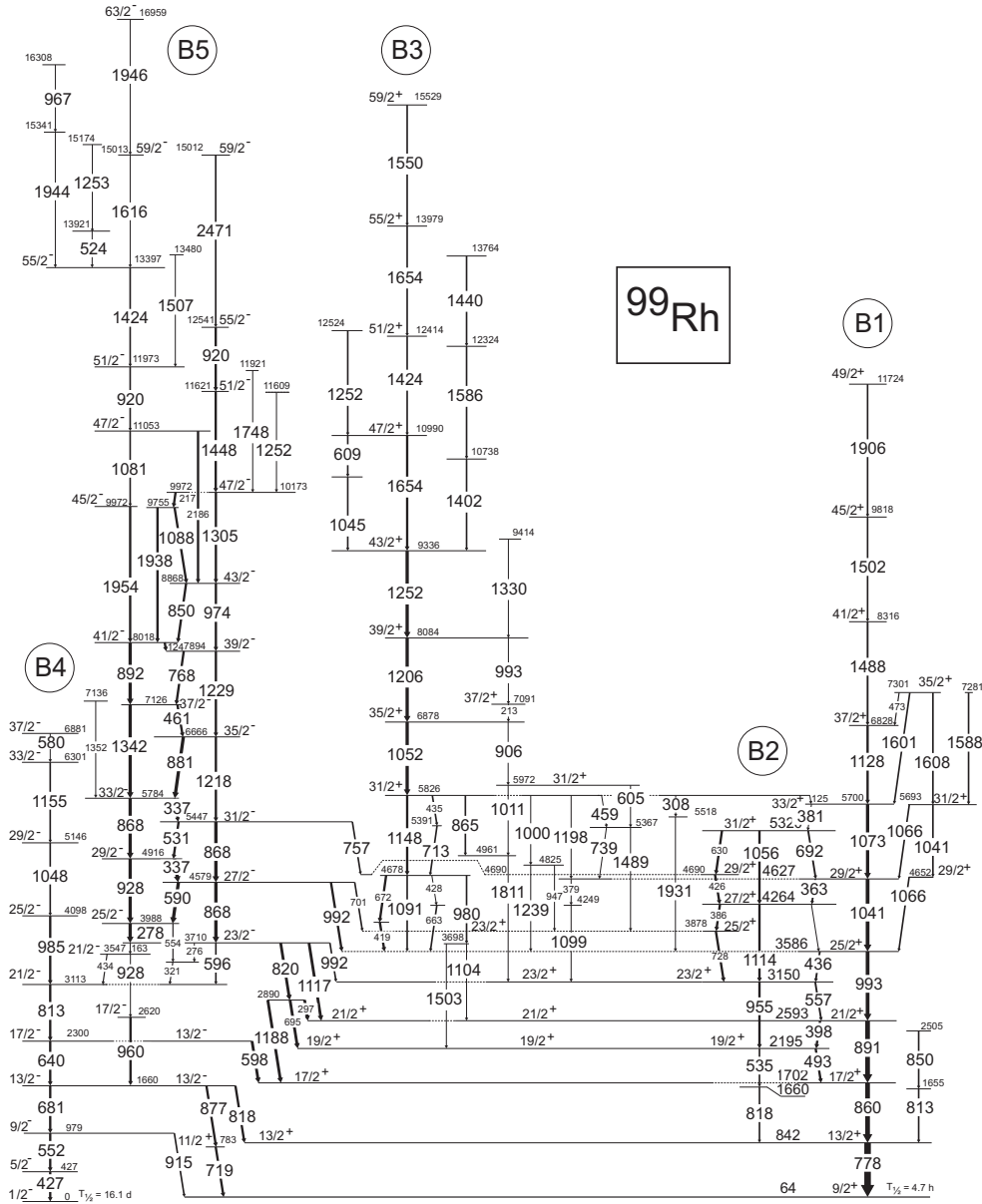


FIG. 2: The level scheme of  $^{99}\text{Rh}$  developed in the present work.

beled B1-B4 could be identified in the present level scheme, which is established up to  $\sim 10$  MeV excitation energy. Similarly fragmentations at the positive parity bands at spins around  $18\hbar$  is observed, which are likely to be

maximally spin aligned states similar to the ones in  $^{101}\text{Rh}$  [28].

## 4. Theoretical calculations and Discussion

### A. Gamma vibrational bands in $A \sim 130$

The energy level spacings (staggering pattern) and transition strengths of gamma vibrational bands provide information regarding the triaxiality of the even-even nuclei in the  $A \sim 130$  mass region [10]. The effect of the coupling of the valance particle on the triaxiality of the even-even core can be studied by a systematic comparison of the gamma bands of even-even nuclei with that of the nearby even-odd or odd-even nuclei. In the present work [12], two bands, namely, B1 and B9 have been observed for the first time. The decay pattern of the band B9, with bandhead spin of  $I^\pi = 15/2^-$ , is found to be quite similar to that of the gamma vibrational band built on the favored signature of the  $\pi h_{11/2}$  band in lighter Cs isotopes [31]. It will be interesting to experimentally identify the states of gamma vibrational band with intermediate spins  $I^\pi = 17/2^-$ ,  $21/2^-$ , etc. The excited states of B1 decay to the band B5 via the  $\Delta I = 1$  transitions with energy higher than 1 MeV. Thus, B1 has been identified as the gamma band coupled with the  $\pi g_{7/2}$  orbital. Similar band structure has not been observed in neighboring odd Cs isotopes [25]. The bandhead of the gamma band coupled with  $\pi g_{7/2}$  orbital is expected to be  $I^\pi = 11/2^+$ . However, the lowest energy state observed in B1 has a spin  $I^\pi = 13/2^+$ . For comparison of the relative level spacings of B1 and B9 with that of the gamma band of neighboring even-even nucleus  $^{130}\text{Xe}$  [11], the  $13/2^+$  state of band B1 and  $15/2^+$  state of band B9 have been normalized to  $3^+$  and  $2^+$  states of that in  $^{130}\text{Xe}$ , respectively (see Figure 3). The gamma band B1 built on  $\pi g_{7/2}$  seems to have the same staggering pattern as that of  $^{130}\text{Xe}$ . At present similar comparison for B9 is not possible as the intermediate levels have not yet been identified. Another negative parity band B15 has been found in the present work, which has level spacing and feeding pattern similar to the favored signature of the  $\pi h_{11/2}$  band as that of B9. Though equivalent band has been

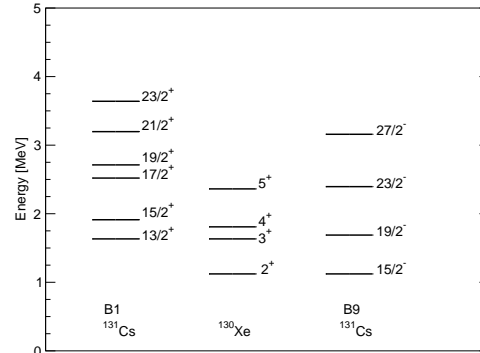


FIG. 3: Comparison of the relative spacing of the experimental levels in gamma bands B1 and B9 of  $^{131}\text{Cs}$  with that of neighboring  $^{130}\text{Xe}$  nucleus. Spins of the different states are marked for each band. The lowest observed states of all these gamma bands are normalized as explained in the text.

identified in  $^{125}\text{Cs}$ , more experimental data in other odd Cs isotopes along with theoretical calculations are required to identify the microscopic structure of B15 type band. It is important to note that through such systematic comparison of the structures of gamma bands coupled with different quasiparticles in even-odd and odd-even nuclei (e.g.,  $^{131}\text{Cs}$ ) one can understand the coupling of the high- $j$  particles to the even-even triaxial core (e.g.,  $^{130}\text{Xe}$ ). This interesting aspect in return would shed more insight to phenomenon like chiral doublet bands in odd-odd nuclei (e.g.,  $^{132}\text{Cs}$ ) which arises from the coupling of a triaxial even-even core with high  $j$  particle and hole.

### B. Octupole collectivity in $A \sim 130$

Neutron deficient isotopes around  $Z = 54$  are predicted to show a softness with respect to octupole deformation at low spin. The signature for such effects are interleaved positive and negative parity bands connected by enhanced E1 transitions. This is due to both proton and neutron levels, arising from the same  $h_{11/2}$  and  $d_{5/2}$  orbitals ( $\pi = -1, \Delta l = \Delta j = 3$ ) being near the Fermi surface. The  $\pi h_{11/2}$ ,  $\pi d_{5/2}$ , and  $\pi g_{7/2}$  bands are seen in the odd-A  $^{117,121-133}\text{Cs}$  isotopes [25]. The

population strength of the  $\pi g_{7/2}$  and  $\pi d_{5/2}$  bands relative to that of the  $\pi h_{11/2}$  band increases considerably with increasing mass number. This happens primarily because the excitation energy of the  $h_{11/2}$  orbital is increasing thus becoming less yrast in the heavier isotopes. These facts are consistent with a decreasing nuclear deformation with increasing mass. Also, in the lighter Cs and I isotopes significant admixture of  $\pi d_{5/2}$  orbitals has been noticed in the  $\pi g_{7/2}$  bands. Features of the  $\pi g_{7/2}$  and  $\pi d_{5/2}$  bands become distinctive in the heavier  $^{127,129,131,133}\text{Cs}$  isotopes. In  $^{131}\text{Cs}$ , these bands are populated with nearly equal strengths, despite the fact that the routhian for band B5 is  $\sim 170$  keV. Similar features have been observed in  $^{127,129,133}\text{Cs}$ . The relative energy of the states in the  $\pi h_{11/2}$  and  $\pi d_{5/2}$  bands in  $^{131}\text{Cs}$  allow  $I \rightarrow I - 1$  E1 transitions. Nevertheless,  $^{131}\text{Cs}$  with  $Z = 55$ ,  $N = 76$ , provides an example of the enhanced octupole correlation arisen from less pronounced pair of octupole-driving orbits, *i.e.*,  $\pi(h_{11/2} \otimes d_{5/2})$  with  $\Omega = 1/2$ . Wave functions are highly localized for lower components; therefore, the octupole-interaction matrix elements (overlaps) between configurations  $h_{11/2}$  and  $d_{5/2}$  can be larger for more stable cases with neutron number around  $N = 76$ .

The  $\Delta I = 1$  connecting E1 transitions are indeed very weak, and further the intensity determination is marred by the presence of doublets. Spectra of the 140.3, 166.6, and 288.2 keV transitions are relatively clean and intensity ratios could be determined. Nevertheless, the presence of these E1 transitions competing with highly collective E2 transitions is already a sign of large B(E1) values. The relative reduced transition probabilities between  $\Delta I = 1$ , E1 and  $\Delta I = 2$ , E2 transitions can be expressed as

$$\frac{B(E1)}{B(E2)} = \frac{1}{1.3 \times 10^6} \frac{E_\gamma^5(E2)}{E_\gamma^3(E1)} \frac{I_\gamma(E1)}{I_\gamma(E2)} [fm^{-2}]$$

where,  $E_\gamma$  is in MeV.

The extracted values of the B(E1)/B(E2) ratios for  $13/2^+$ ,  $17/2^+$ , and  $21/2^+$  levels

are  $1.54 \times 10^{-8}$ ,  $2.74 \times 10^{-8}$ , and  $1.34 \times 10^{-8}$  [ $fm^{-2}$ ], respectively. Based on the deformation of the even-even core  $^{130}\text{Xe}$  [32], the B(E1) values for the  $^{131}\text{Cs}$  have been estimated to be around  $\sim 6.0 \times 10^{-5}$  *W.u.*, indicating a similar enhancement of octupole correlation in this nucleus.

### C. Octupole collectivity in $A \sim 100$

Excited states in the  $^{98}\text{Rh}$ ,  $^{99}\text{Rh}$  and  $^{99}\text{Pd}$  nuclei were populated through the  $^{75}\text{As}(^{28}\text{Si}, \text{xpyn})$  fusion-evaporation reaction at  $E_{lab} = 120$  MeV and the deexcitations were investigated using in-beam  $\gamma$ -ray spectroscopic techniques involving Compton-suppressed clover detector array. The level structures observed in  $^{99}\text{Pd}$  have been interpreted in the framework of a microscopic theory based on the deformed Hartree-Fock (HF) and angular momentum projection techniques. Various bands are reproduced with the configurations  $\nu(g_{7/2})^m \otimes \nu(d_{5/2})^n \otimes (\nu h_{11/2})^q 4 \otimes (\pi g_{9/2})^{-r}$ . As the  $\nu h_{11/2}$  and  $\nu d_{5/2}$  orbitals with ( $\Delta l=3$ ) being near the Fermi surface in this mass region. The signature for such effects are interleaved positive and negative-parity bands connected by enhanced E1 transitions. Such E1 transitions between the levels of  $\nu h_{11/2}$  band (B3) to  $\nu d_{5/2}$  band (B2) have been observed in the present work. This is because both the neutron  $h_{11/2}$  and  $d_{5/2}$  orbitals ( $\pi = -1$ ,  $\Delta l = \Delta j = 3$ ) are near the Fermi surface. Nevertheless, the presence of these E1 transitions competing with highly collective E2 transitions is already a sign of large B(E1) values. The  $\Delta I=1$  connecting E1 transitions are intense in this nucleus. Spectra of the 1056.3, 974.1, and 1379.2 keV transitions are relatively clean and intensity ratios could be determined (Figure 1). The relative reduced transition probabilities between  $\Delta I=1$ , E1 and  $\Delta I = 2$ , E2 transitions can be expressed as

$$\frac{B(E1)}{B(E2)} = \frac{1}{1.3 \times 10^6} \frac{E_\gamma^5(E2)}{E_\gamma^3(E1)} \frac{I_\gamma(E1)}{I_\gamma(E2)} [fm^{-2}]$$

where,  $E_\gamma$  is in MeV. The extracted values of the B(E1)/B(E2) ratios for  $15/2^-$ ,  $19/2^-$ , and  $23/2^-$  levels are  $14.7 \times 10^{-8}$ ,  $13.8 \times 10^{-8}$  and  $8.7 \times 10^{-8}$  [ $fm^{-2}$ ] respectively [15].

### Acknowledgments

Author acknowledge the joint effort of IUAC, New Delhi, TIFR, Mumbai, and IUC-DAEF and SINP, Kolkata, in establishing the INGA clover array. Thanks to the pelletron staff for smooth functioning of the accelerator. The help of all the collaborators of the above works are gratefully acknowledged.

### References

- [1] J. Cederkl *et al.*, Eur. Phys. J. A 1, 17 (1998).
- [2] J. Cederkl *et al.*, Z. Phys. A 359, 227 (1997).
- [3] B.M. Nyak *et al.*, Phys. Rev. C 60, 024307 (1999).
- [4] J. Gizon *et al.*, Phys. Rev. C 59, R570 (1999).
- [5] W.F. Piel *et al.*, Phys. Rev. C 15, 287 (1977).
- [6] J. Dubuc *et al.*, Phys. Rev. C 37, 1932 (1988).
- [7] S. Chattopadhyay *et al.*, Phys. Rev. C 57, R471 (1998)
- [8] S.S. Ghugre *et al.*, Phys. Rev. C 58, 3243 (1998).
- [9] R.P. Singh *et al.*, Eur. Phys. J A 7, 35 (2000).
- [10] E.A. McCutchan *et al.*, Phys. Rev. C 76, 024306 (2007).
- [11] L. Goettig *et al.*, Nucl. Phys. A357, 109 (1981).
- [12] S. Sihotra *et al.*, Phys. Rev. C 78, 034313 (2008).
- [13] R. Kumar *et al.*, Phys. Rev. C 72, 044319 (2005).
- [14] K. Higashiyama and N. Yoshinaga, Prog. of Theoretical Physics, 120, 525 (2008).
- [15] S. Sihotra *et al.*, Phys. Rev. C 83, 024313 (2011).
- [16] R. K. Bhowmik, S. Muralithar, and R. P. Singh, DAE Symposium on Nucl Phys., 44B, 422 (2001).
- [17] D. C. Radford, Nucl. Instrum. and Methods A 361, 306 (1995).
- [18] K. Starosta *et al.*, Nucl. Instrum. Meth. Phys. A 423, 16 (1999).
- [19] G. Ripka, *Advances in Nuclear Physics*, Vol. 1 (1966) Ed. M. Baranger and E. Vogt (Plenum).
- [20] R. E. Peierls and Y. Yoccoz, Proc. Phys. Soc. A 70, 381 (1957).
- [21] C. R. Praharaaj, J. Phys. G 14, 843 (1988).
- [22] A. Faessler, P. Plastino, and S. A. Moszkowski, Phys. Rev. 156, 1064 (1967).
- [23] Z. Naik and C. R. Praharaaj, Phys. Rev. C 67, 054318 (2003).
- [24] S. Frauendorf, Nucl. Phys. A557, 259c (1993).
- [25] S. Sihotra *et al.*, Phys. Rev. C 79, 044317 (2009).
- [26] A.Y. Deo *et al.*, Phys. Rev. C 79, 067304 (2009).
- [27] S. Sihotra *et al.*, Phys. Rev. C 43, 45 (2010).
- [28] J. Timár *et al.*, Nucl. Phys. A696, 241 (2001).
- [29] S. Sihotra in Manuscript Under Process.
- [30] J. Gizon *et al.*, Phys. Rev. C 59, R570 (1999).
- [31] Y. Liang, R. Ma, E.S. Paul, N. Xu, D.B. Fossan, and R.A. Wyss, Phys. Rev. C 42, 890 (1990).
- [32] S. Raman *et al.*, At. Data Nucl. Data Tables 36, 1 (1987).